SPE
Society of Petroleum Engineers

SPE 16342

A Versatile, Fully Implicit, Black Oil Simulator With Variable Bubble-Point Option

by K.L. Farnstrom and T. Ertekin, Pennsylvania State U.

SPE Members

This paper was prepared for presentation at the SPE California Regional Meeting held in Ventura, California, April 8-10, 1987.

ABSTRACT

A stable and efficient, general-purpose, variable bubble point black oil simulator is presented. The program utilizes the method of substitution of variables for modeling gas phase appearance and disappearance. Paralleling its application in conventional reservoir simulation, recent work has shown that the present model forms a solid basis for the development of more specialized simulators containing unique options.

The objective of this paper is to present a general description of the simulator and to describe in detail the numerical methods and specific programming techniques utilized. At the heart of the model is the variable bubble point formulation. This employs relatively complex Jacobian building routines and switching schemes. These are specially designed for efficiency and acceleration of convergence.

The automatic timestep selector for thermal simulation presented by Sammon and Rubin has been modified to accommodate the substitution of variables in black oil simulation. Techniques for implementation of this timestep selector are presented.

To solve the system of nonlinear flow equations, a modified Newton-Raphson procedure is presented. In comparison with the classical Newton-Raphson procedure, the present method requires a larger number of iterations per time step, but overall computation time is significantly reduced. A series of tests are presented to compare the classical and the modified Newton-Raphson procedures and to illustrate the efficiency and stability of the model.

INTRODUCTION

The literature contains numerous references to the method of substitution of variables for modeling phase appearance and disappearance in black oil and thermal simulation[1-7]. Often equations and partial segments of the method are presented, however, important details are absent. One of the objectives of this paper is to provide a comprehensive outline of formulations, switching schemes, and techniques for accelerating convergence in the substitution of variables method. This presentation applies to general-purpose fully implicit black oil simulators, however, our research shows that the methods presented in this paper are suitable for application to more specialized problems in black oil simulation. They have been successfully implemented in the simulation of immiscible polymer flooding[8], and the simulation of water and gas injection schemes for naturally and hydraulically fractured reservoirs.

An effective automatic timestep selector was presented by Sammon and Rubin[9] for thermal simulation. We present procedures to adapt this timestep selection routine to variable bubble point black oil problems. Techniques are described which enable the routine to operate in conjunction with the substitution of variables method.

A modified Newton-Raphson procedure[10] is presented as an accelerated solution technique for the fully implicit scheme. The modified procedure is novel in its approach and provides significant time savings when used in place of the classical Newton-Raphson procedure. A version of the modified procedure is presented for use with gas phase appearance and disappearance and the method of substitution of variables.

THE FULLY IMPLICIT SCHEME

The basic principles of fully implicit three phase black oil simulation are widely documented in the literature. For simplicity, only a brief summary is presented here. Details specific to the method of substitution of variables are noted.

References and illustrations at end of paper.

The continuity equation is used to define a residual vector having the general form

$$R = \frac{\Delta M}{\Delta t} - \Delta[\lambda \Delta \Phi] + Q \tag{1}$$

If the principle of conservation of mass is applied at any instant in time, Equation (1) can be set equal to zero.

$$R = 0 \tag{2}$$

Equation (1) can be written to express the residual in the j^{th} reservoir cell as a three component vector comprised of the residuals for the water, oil, and gas phases.

$$R_j = \begin{bmatrix} R_w \\ R_o \\ R_g \end{bmatrix}_j \tag{3}$$

The residuals may be expressed as a function of a solution vector X, and it follows that

$$R(X) = 0 \tag{4}$$

The vector X is comprised of the primary variables from each reservoir cell. Primary variables are selected to provide maximum information on cell conditions. The substitution of variables method utilizes two sets of primary variables based on the presence or absence of the free gas phase. When free gas is present in the j^{th} reservoir cell, the solution vector utilizes the primary variables S_w, S_o, and P_o and therefore assumes the form

$$X_j = \begin{bmatrix} S_w \\ S_o \\ P_o \end{bmatrix}_j \tag{5}$$

In the absence of the free gas phase, the solution vector utilizes the primary variables R_s, S_o, and P_o and has the form

$$X_j = \begin{bmatrix} R_s \\ S_o \\ P_o \end{bmatrix}_j \tag{6}$$

Newton's method is applied to obtain a solution for the system of nonlinear equations generated by Equation (4). Newton's method may be expressed as

$$R(X^v+\Delta X) \cong R(X^v) + \left(\frac{\partial R}{\partial X}\right)^v \Delta X \tag{7}$$

The term $\frac{\partial R}{\partial X}$ represents the derivatives of the residual with respect to the primary variables of the solution vector X. These derivatives are arranged into a matrix known as the Jacobian. When the free gas phase is present in the j^{th} reservoir cell, the Jacobian has the form

$$\left(\frac{\partial R}{\partial X}\right)_j = J_j = \begin{bmatrix} \frac{\partial R_w}{\partial S_w} & \frac{\partial R_w}{\partial S_o} & \frac{\partial R_w}{\partial P_o} \\ \frac{\partial R_o}{\partial S_w} & \frac{\partial R_o}{\partial S_o} & \frac{\partial R_o}{\partial P_o} \\ \frac{\partial R_g}{\partial S_w} & \frac{\partial R_g}{\partial S_o} & \frac{\partial R_g}{\partial P_o} \end{bmatrix}_j \tag{8}$$

In the absence of the free gas phase, the Jacobian has the form

$$\left(\frac{\partial R}{\partial X}\right)_j = J_j = \begin{bmatrix} \frac{\partial R_g}{\partial R_s} & \frac{\partial R_g}{\partial S_o} & \frac{\partial R_g}{\partial P_o} \\ \frac{\partial R_o}{\partial R_s} & \frac{\partial R_o}{\partial S_o} & \frac{\partial R_o}{\partial P_o} \\ \frac{\partial R_w}{\partial R_s} & \frac{\partial R_w}{\partial S_o} & \frac{\partial R_w}{\partial P_o} \end{bmatrix}_j \tag{9}$$

Note that the ordering of equations is reversed in (8) and (9). This is necessary to insure that the Jacobian remains well conditioned for both sets of primary variables.

To apply Newton's method, the linear equation

$$J^v \Delta X = - R(X^v) \tag{10}$$

is written for the entire reservoir using the most recent values available for X and then solved with suitable techniques for values of ΔX. The solution vector is then updated using

$$X^{n+1} = X^v + \Delta X \tag{11}$$

Next, the residual and the Jacobian are re-evaluated and Equation (10) is again solved for values of ΔX. Iteration continues until values of ΔX approach zero. At this point, a solution has been obtained for the primary variables at the new time level $t + \Delta t$. Additional reservoir parameters may then be calculated for the new time level using appropriate equations and the values of X.

VARIABLE BUBBLE POINT FORMULATION METHOD OF SUBSTITUTION OF VARIABLES

Modeling appearance and disappearance of the free gas phase is a formidable problem in black oil simulation. Two fundamentally different methods[1] have evolved: the pseudogas approach[11], and the substitution of variables method[2].

The literature contains numerous references to the substitution of variables method[1-7]. Often equations and partial segments of the technique are provided, however, important details are absent. In the following sections, a comprehensive outline is presented of formulations, switching schemes, and

techniques for accelerating convergence in the substitution of variables method.

Routines for construction of the Jacobian are at the heart of the Newton-Raphson procedure. As noted in the previous section, two independent sets of primary variables are required for modeling reservoir performance in the presence and absence of the free gas phase. Two sets of primary variables require the coding of two separate Jacobian building routines, and a number of supportive routines must also be coded in dual form. In addition, extra code is required to accommodate the transition of reservoir cells across the bubble point and to accommodate upstream weighting of transmissibilities when adjacent cells are on opposite sides of the bubble point. These additions make the substitution of variables method lengthy to program, however, it is more realistic and provides somewhat more accurate results than its alternative, the pseudogas approach[1].

The rate of convergence of the fully implicit Newton-Raphson procedure is extremely sensitive to minor programming inaccuracies and omissions. Therefore, Jacobian building routines and switching schemes for crossing the bubble point require careful design to obtain maximum efficiency and stability.

In the following sections, techniques will be presented for Jacobian construction. Four separate routines are required for derivatives of the accumulation terms. Two routines each are required for derivatives of the interblock flow and source terms. The use of two indicator arrays is presented. The purpose of these is to record the status of the free gas phase in each reservoir cell, to route execution through proper routines, and to facilitate the switching of variables during phase appearance and disappearance. The arrays are named INDC1 and INDC2. The dimension of each indicator array is set equal to the number of cells in the reservoir. Each reservoir cell is assigned one entry in each array. INDC1 is used with calculations of the interblock flow and source terms, and INDC2 is used in conjunction with the accumulation terms.

Derivatives of the Accumulation Terms

The finite difference approximation for the accumulation term may be written in the general form

$$\frac{V_b}{\Delta t}\frac{\partial}{\partial t}\left(\frac{SR_s\phi}{B}\right) \cong \frac{V_b}{\Delta t}\Delta_t\left(\frac{SR_s\phi}{B}\right) \qquad (12)$$

Based upon cell conditions, four separate expansions of this equation are required. The following possibilities exist for a typical reservoir cell:

(1) Free gas is present for the duration of the timestep.

(2) Free gas is present at the beginning, but disappears during the timestep.

(3) No free gas is present for the duration of the timestep.

(4) No free gas is present at the beginning, but the free gas phase appears during the timestep.

The modeling of the four cases requires four separate routines. Each of these routines uses a different expansion of Equation (12).

In the discussion which follows, expansions of Equation (12) are presented in terms of the gas equation. Additional terms are presented for the oil, gas and water residuals when necessary. In these equations, if the free gas phase is present in the cell, R_s and B_o are functions of P_o. If the free gas phase is absent, R_s is a function of the bubble point pressure, P_b, and B_o is a function of both P_b and P_o. Porosity, B_w, and B_g are considered as functions of P_o only.

Routines for the four cases are presented in detail below, and a brief summary is shown in Figure 1. INDC2 is used in the selection and switching of the four routines and is assigned the values 1 through 4 based on conditions present in each reservoir cell. Switches are made in the values of INDC2 whenever cells cross the bubble point.

Case 1. During the timestep, pressure within the reservoir cell remains below the bubble point. The expansion of Equation (12) takes the general form

$$\begin{aligned}\Delta_t\left(\frac{S_oR_s\phi}{B_o}\right) &= \left(\frac{R_s\phi}{B_o}\right)^{n+1}\Delta_tS_o \\ &+ S_o^n\left(\frac{\phi}{B_o}\right)^{n+1}\left(\frac{R_s^{n+1}-R_s^n}{P_o^{n+1}-P_o^n}\right)\Delta_tP_o \\ &- \left(\frac{S_oR_s}{B_o}\right)^n\left(\frac{\phi}{B_o}\right)^{n+1}\left(\frac{B_o^{n+1}-B_o^n}{P_o^{n+1}-P_o^n}\right)\Delta_tP_o \\ &+ \left(\frac{S_oR_s}{B_o}\right)^n\left(\frac{\phi^{n+1}-\phi^n}{P_o^{n+1}-P_o^n}\right)\Delta_tP_o \end{aligned} \qquad (13)$$

The primary variables remain S_w, S_o, and P_o for the duration of the timestep. INDC2 is assigned the value 1 for reservoir cells using Equation (13).

Case 2. During the timestep, pressure within the cell increases from below to above the bubble point. All free gas goes into solution in the oil phase. The primary variables at the beginning of the timestep are S_w, S_o, and P_o, but must be switched to R_s, S_o, and P_o upon disappearance of the free gas phase. This switch generally occurs after one or possibly two iterations when the simulator attempts to place more gas into solution than is available in the cell. At this time, the summation of S_o and S_g becomes greater than or equal to 1.0, and S_g is calculated as zero or a negative number.

The simulator begins the timestep using Equation (13). Once the free gas phase disappears in the cell, subsequent iterations are completed using the following expansion:

$$\Delta_t\left(\frac{S_oR_s\phi}{B_o}\right) =$$

$$\left(\frac{R_s\phi}{B_o}\right)^{n+1}\Delta_t S_o + S_o^n\left(\frac{\phi}{B_o}\right)^{n+1}\Delta_t R_s$$

$$-\left(\frac{S_o R_s}{B_o}\right)^n\left(\frac{\phi}{B_o}\right)^{n+1}\left(\frac{B_{o_b}^{n+1}-B_{o_b}^n}{P_b^{n+1}-P_b^n}+C_o\right)$$

$$\left(\frac{P_b^{n+1}-P_b^n}{R_s^{n+1}-R_{s_b}^n}\right)\Delta_t R_s^*$$

$$+\left(\frac{S_o R_s}{B_o}\right)^n_b\left(\frac{\phi}{B_o}\right)^{n+1}C_o\Delta_t P_o^*$$

$$+\left(\frac{S_o R_s}{B_o}\right)^n\left(\frac{\phi^{n+1}-\phi^n}{P_o^{n+1}-P_o^n}\right)\Delta_t P_o \qquad (14)$$

Because free gas is present in the cell at time level n, the following derivatives for the free gas phase must be included in the Jacobian:

$$-\left(\frac{\phi}{B_g}\right)^{n+1}\Delta_t S_o - \left(\frac{S_g}{B_g}\right)^n\left(\frac{\phi}{B_g}\right)^{n+1}\left(\frac{B_g^{n+1}-B_g^n}{P_o^{n+1}-P_o^n}\right)\Delta_t P_o$$

$$+\left(\frac{S_g}{B_g}\right)^n\left(\frac{\phi^{n+1}-\phi^n}{P_o^{n+1}-P_o^n}\right)\Delta_t P_o$$

These terms represent the free gas saturation in the cell at time level n. They are added to Equation (14) to complete the derivatives of the gas equation for the cell. Additional terms must also be included in the residuals of the water, oil, and gas equations as shown below:

Water Residual:

$$ARWE = \frac{V_b}{\Delta t}\left(\frac{\phi}{B_w}\right)^{n+1}S_g^n \qquad (15)$$

Oil Residual:

$$AROE = \frac{V_b}{\Delta t}S_o^n\,\phi^{n+1}\left(\frac{1}{B_{o_b}^n}-\frac{1}{B_o^n}\right) \qquad (16)$$

Gas Residual:

$$ARGE = R_s^n AROE - \frac{V_b}{\Delta t}\left(\frac{\phi}{B_g}\right)^{n+1}(S_w^{n+1}-S_w^n) \qquad (17)$$

The effect of placing these additional terms in the residuals is to shift cell conditions to the bubble point. The bubble point is calculated as a function of the value of R_s from the most recent iterate. The following iterations are then completed using the slope (2-3) of Figure 2, rather than the chord slope (1-3). This technique significantly accelerates convergence of the Newton-Raphson scheme as nonlinearities are reduced. At the end of each iteration, bubble points are recalculated, additions to the residuals are improved, and the slope (2-3) is again utilized in the Jacobian.

As shown in Figure 1, the value of INDC2 is set equal to 1 at the beginning of the timestep. During the first several iterations, the free gas phase disappears, and the value of INDC2 is reset to 2 to route execution through routines utilizing Equations (14) through (17). The routine for Case 2 will then be executed until convergence is attained.

Case 3. During the timestep, pressure within the reservoir cell remains greater than the bubble point. All available gas remains in solution in the oil phase, and the expansion of Equation (12) takes the form:

$$\Delta_t\left(\frac{S_o R_s\phi}{B_o}\right) = \left(\frac{R_s\phi}{B_o}\right)^{n+1}\Delta_t S_o + S_o^n\left(\frac{\phi}{B_o}\right)^{n+1}\Delta_t R_s$$

$$-\left(\frac{S_o R_s}{B_o}\right)^n\left(\frac{\phi}{B_o}\right)^{n+1}\left(\frac{B_{o_b}^{n+1}-B_{o_b}^n}{P_b^{n+1}-P_b^n}+C_o\right)$$

$$\left(\frac{P_b^{n+1}-P_b^n}{R_s^{n+1}-R_s^n}\right)\Delta_t R_s + \left(\frac{S_o R_s}{B_o}\right)^n\left(\frac{\phi}{B_o}\right)^{n+1}C_o\Delta_t P_o$$

$$+\left(\frac{S_o R_s}{B_o}\right)^n\left(\frac{\phi^{n+1}-\phi^n}{P_o^{n+1}-P_o^n}\right)\Delta_t P_o \qquad (18)$$

The primary variables remain R_s, S_o, and P_o for the duration of the timestep. INDC2 has the value of 3 to route execution through routines utilizing Equation (18).

Case 4. During the timestep, the free gas phase appears in the reservoir cell. This appearance may be the result of a decline in cell pressure from above to below the bubble point, or due to injection of free gas into the cell. The primary variables at the beginning of the timestep are R_s, S_o, and P_o, but are switched to S_w, S_o, and P_o when the free gas phase appears. This switch occurs typically within the first two iterations of the timestep, when calculated values of R_s^{n+1} exceed the values of $R_s(P_o^{n+1})$ from tabulated PVT data.

The simulator begins the timestep executing above the bubble point. Once the criteria for free gas appearance are satisfied, strong nonlinearities are introduced because B_o^n, B_o^{n+1}, R_s^n, and R_s^{n+1} exist on opposite sides of the inflection points in Figure 3. The solution may be gained through iterations along the chord slopes (1-3). A more stable and efficient technique is to move conditions at time level n to the bubble point and iterate with tangents along the slope (2-3)[3].

The simulator begins the timestep using Equation (18). Once free gas appears in the cell, subsequent iterations are completed using the expansion:

$$\Delta_t \left(\frac{S_o R_s \phi}{B_o}\right) = \left(\frac{R_s \phi}{B_o}\right)^{n+1} \Delta_t S_o$$

$$+ S_o^n \phi^{n+1} \left(\frac{R_s^{n+1}}{B_o^{n+1}} - \frac{R_s^n}{B_{o_b}^n}\right) \frac{1}{P_o^{n+1} - P_b^n} \Delta_t P_o^*$$

$$+ \left(\frac{S_o R_s}{B_o}\right)^n \left(\frac{\phi^{n+1} - \phi^n}{P_o^{n+1} - P_o^n}\right) \Delta_t P_o \qquad (19)$$

Cell conditions are moved to the bubble point by addition of the following terms to the residuals of the oil and gas equations:

Oil Equation:

$$AROE = \frac{V_b}{\Delta t} S_o^n \phi^{n+1} \left(\frac{1}{B_{o_b}^n} - \frac{1}{B_o^n}\right) \qquad (20)$$

Gas Equation:

$$ARGE = R_s^n AROE \qquad (21)$$

As shown in Figure 1, INDC2 has the value of 3 at the beginning of the timestep. Upon appearance of the free gas phase, the value of INDC2 is reset to 4 to route execution through Equations (19) through (21). The routine for Case 4 is then utilized for the cell until convergence is attained.

Derivatives of the Interblock Flow Terms

Numerical differentiation is typically used for the interblock flow derivatives. Two parallel sections of code are necessary, one for each set of primary variables. Unlike the derivatives of the accumulation terms, no additional derivatives are necessary for crossing the bubble point.

Single point upstream weighting is utilized for calculation of transmissibilities. Complications occur when the downstream reservoir cell requires a different set of primary variables from the upstream cell. Examples are: during production when a cell containing free gas is adjacent to a higher pressure cell containing no free gas, and during gas injection when a cell containing no free gas is adjacent to a higher pressure cell containing the free gas phase. In these and other situations, a different set of primary variables is required for upstream and downstream cells.

This problem can be overcome as follows:

(1) The derivatives of the transmissibilities are calculated with respect to the primary variables in effect in the upstream cell.

(2) The transmissibilities in the interblock flow term of residual are calculated using conditions in the upstream cell.

(3) The ordering of equations in the construction of the Jacobian is based on conditions in the central cell (w,o,g vs. g,o,w).

Six separate routines will be required to calculate derivatives of the interblock flow terms for all possible combinations of upstream weighting (see Figure 4). INDC1 serves as a useful guide in selection of the proper routine. The value of INDC1 in the central gridblock, the position of the upstream cell, and the value of INDC1 in the upstream cell provide sufficient information for selection of the proper routine.

Derivatives of the Source Terms

Numerical differentiation is typically used for the derivatives of the source terms. The calculation of these derivatives is straightforward. Two parallel routines are required, one for each set of primary variables. The proper routine is selected based on the value of INDC1 (see Figure 5).

Initialization and Switching

At the start of each timestep, the values of INDC1 and INDC2 are initialized for all reservoir cells. Only two choices are available. If the free gas phase is present, INDC1=1 and INDC2=1. If no free gas is present in a cell, INDC1=0 and INDC2=3 (see Figure 6).

At the time of initialization, it is convenient to calculate quantities required by the variable bubble point routines. $R_{s_b}^n$ is the value of R_s at saturation pressure. For cells containing free gas, the value of $R_{s_b}^n$ is calculated by placing all free gas into solution[4] in the oil phase.

$$R_{s_b}^n = R_s^n + \left(\frac{S_g B_o}{S_o B_g}\right)^n \qquad (22)$$

This quantity is utilized during simulation of gas phase disappearance. P_b^n and $B_{o_b}^n$ are determined using $R_{s_b}^n$ and tabulated PVT data.

During a timestep, no change is made in indicators or primary variables unless phase appearance or disappearance occurs. Phase changes are determined using the switching criteria shown in Figure 7. Switching schemes exchange primary variables and reassign indicators, and in the case of gas phase disappearance, values of S_o^{n+1}, R_s^{n+1}, and S_g^{n+1} are reset to expedite convergence. The new values for indicators will route execution through appropriate routines for the new primary variables and complete the transition across the bubble point.

When gas phase disappearance occurs, the summation of S_o^{n+1} and S_w^{n+1} is typically greater than 1.0, and S_g^{n+1} is less than zero. This occurs because the simulator attempts to place more free gas into solution than is available in the cell. The value of S_o^{n+1} should therefore be improved using the equation

$$S_o^{n+1} = 1.0 - S_w^{n+1} \qquad (23)$$

An accurate approximation of R_s^{n+1} is then calculated using the new value of S_o^{n+1} and the value of S_g^{n+1}.

$$R_{s_{improved}}^{n+1} = R_s^{n+1} + \left(\frac{S_g B_o}{S_o B_g}\right)^{n+1} \qquad (24)$$

The value of S_g^{n+1} is then reset to zero. The new values for S_o^{n+1} and R_s^{n+1} improve convergence.

As previously stated, appearance or disappearance of the free gas phase happens typically during the first or sometimes the second iteration of a timestep. Occasionally a large section of gridblocks will cross the bubble point all at once. When this occurs, a few more gridblocks may also cross. These extra blocks will be located along the margins of the group, and conditions in these blocks will be very close to the bubble point. As the solution is improved in successive iterations, the extra blocks will be switched back across the bubble point. The necessary code to accomplish this switching is included in Figure 7. INDC1, INDC2, and the primary variables are reset to the original values used at the start of the timestep.

AUTOMATIC TIMESTEP CONTROL

An effective error driven timestep selection scheme for thermal simulation was presented by Sammon and Rubin[9]. The purpose of their scheme is to restrict the time truncation error which results from the backwards difference approximation of the time derivative in the continuity equation. This is done by calculation of a timestep size which is based upon restriction of the time truncation error rather than based upon maximum specified changes in reservoir variables. This scheme has been implemented with several modifications and adaptations to accommodate the substitution of variables in black oil simulation. The development by Sammon and Rubin is lengthy and will not be repeated here. The present discussion will center on modifications.

In the presentation by Sammon and Rubin, an error controlled timestep is calculated based on the data from the previous timestep using the equation:

$$\Delta t^{n+2} = 2\varepsilon / \sqrt{||\dot{X}_b^{n+1} - \dot{X}_c^{n+1}||/\Delta t^{n+1}} \qquad (25)$$

In Equation (25) ε is a user supplied error parameter. $\dot{X}_c^{n+1}$ is a vector whose components define the correct or actual time rate of change of the solution vector for the previous timestep. $\dot{X}_b^{n+1}$ is a vector whose components define the approximate time rate of change of the solution vector as determined using the backward difference formula. $\dot{X}_c^{n+1}$ is calculated from the matrix equation:

$$DA(X^{n+1})\ \dot{X}_c^{n+1} = F(X^{n+1}) \qquad (26)$$

and $\dot{X}_b^{n+1}$ is calculated from the matrix equation

$$[DA(X^{n+1}) - \Delta t^{n+1}\ DF(X^{n+1})]\ \dot{X}_b^{n+1} = \left(\frac{1}{\Delta t^{n+1}}\right)(A(X^{n+1}) - A(X^n)) \qquad (27)$$

The matrix in square brackets is the Jacobian constructed during the last iteration of the previous timestep.

Equation (27) is modified slightly to utilize the Jacobian presented in this paper for black oil simulation. The following expression is obtained:

$$[DF(X^{n+1}) - \frac{DA(X^{n+1})}{\Delta t^{n+1}}]\ \dot{X}_b^{n+1} = \frac{-1}{(\Delta t^{n+1})^2}\ (A(X^{n+1}) - A(X^n)) \qquad (28)$$

The term in square brackets is the Jacobian presented in Equation (10). This Jacobian is available in inverted form from the last iteration of the previous timestep and is used in conjunction with a new right-hand side vector for calculation of $\dot{X}_b^{n+1}$.

In calculation of the error controlled timestep, several considerations are necessary to accommodate the substitution of variables technique. For each set of primary variables, separate routines are required for calculating and loading matrix terms in Equations (26) and (27). Dual routines are necessary for calculation of the vector norm by the following equation:

$$||e|| = \max_{1<i<m*N} (|e_i|/\alpha_i) \qquad (29)$$

For each primary variable i, the weight α_i is assigned a specific value. For saturations, S_o and S_w, α_i equals 1.0. For R_s and P_o, α_i is calculated from

$$\alpha_{R_s} = \omega R_{s_{max}} \qquad \alpha_{P_o} = \omega P_{o_{max}} \qquad (30)$$

ω is equal to a user supplied fraction. $R_{s_{max}}$ and $P_{o_{max}}$ are the maximum reservoir values of R_s and P_o from the preceding timestep.

An algorithm is presented by Sammon and Rubin[9] for prediction of phase appearance and disappearance for the upcoming timestep. This enables timestep sizes to be reduced as necessary in thermal simulation, and increases the reliability of the simulator during phase changes. No significant stability problems or timestep restrictions were experienced with the substitution of variables technique presented in this paper. Therefore, it is not recommended that timestep sizes be reduced on the basis of phase appearance and disappearance during black oil simulation.

Another useful algorithm is presented by Sammon and Rubin[9] for prediction of results for succeeding timesteps. The technique uses the time rate of change of primary variables from the previous timestep to estimate changes in the primary variables for the current timestep. Using this algorithm, a routine has been prepared to operate in conjunction with the method of substitution of variables. Not only are predictions made for the values of primary variables, but predictions are also made for phase appearance and disappearance.

Dual routines are written to accommodate both sets of primary variables. Using the algorithm, estimates are made for the first iteration values of the initial primary variables. Next, these values are

subjected to the same switching criteria as presented in Figure 7. If S_g^{n+1} < EPSGAS, then phase disappearance is predicted for the cell, and all subsequent calculations and switches are completed in preparation for phase disappearance. If $R_s^{n+1} > R_s(P_o^{n+1})$ - EPSRST, then gas phase appearance is predicted, and all necessary switching is completed in preparation for phase appearance in the cell (see Figure 7).

The estimation procedure has several important advantages. Cells which will be crossing the bubble point during the timestep are identified, all preparatory calculations and switches are completed for these cells, and accurate estimates are made for the values of the primary variables prior to the actual beginning of iteration.

MODIFIED NEWTON-RAPHSON (MNR) PROCEDURE

Reduction in computation time is a major goal in fully implicit simulation. This is typically achieved through techniques which accelerate convergence of the Newton-Raphson scheme and reduce the number of iterations per time step. The technique presented here achieves significant time savings in a different way. It actually increases the total number of iterations required per timestep, but overall execution time is reduced through larger savings in the average time required per iteration.

To understand reasons for the success of the new technique, it is instructive to compare the execution times for different segments of the standard Newton-Raphson procedure. For our purposes, a standard Newton-Raphson iteration will be divided into four segments: computation of the Jacobian entries and the right-hand side vector, loading the Jacobian bands into an envelope, inverting the Jacobian, and solving the system of linear equations using the prescribed right-hand side vector. Table 1.a contains a comparison of the times required for completion of each of these four segments. Times are presented for a 5x5, an 8x8, and a 10x10 grid system. In these examples, standard ordering and matrix inversion by standard elimination are used.

From the data, several observations are evident. By a wide margin, matrix inversion requires the largest expenditure in time. Also, time requirements for inversion increase drastically with an increase in grid size. The construction and loading of Jacobian entries are relatively more important for smaller grids. As grid dimensions increase, time requirements for Jacobian construction and loading become trivial in comparison with requirements for matrix inversion.

The modified Newton-Raphson procedure (MNR) presented here gains large savings in time by omission of Jacobian construction, loading, and inversion in 50 percent or more of the iterations per timestep. Several options are available to the user. Overall results vary according to option chosen, grid dimensions, and reservoir conditions. Large savings in execution time, in the range of 40 to 50 percent per timestep are common. Table 1.b contains execution times for the shortened MNR iterations. Times are presented for the three grid sizes. The use of the shortened iterations is described in the following section.

Description of the Procedure

The MNR procedure uses only periodic updating and inversion of the Jacobian. The technique employs two basic types of iterations:

Type (1): The full iteration as previously described. This iteration includes all of the steps shown in Table 1.a. During the full Newton iteration, a copy of the inverted Jacobian must be saved.

Type (2): The modified Newton iteration which includes:

A. Calculation of an updated residual using the solution vector from the previous iteration.

B. Solution of the system of equations for the reservoir using the updated residual and the inverted Jacobian from a previous Type (1) iteration.

The two basic types of iterations may be combined in several ways. These combinations are known as options. Three options are presented.

Option (1): The solution scheme alternates between the use of Type (1) and Type (2) iterations. The timestep always begins with a Type (1) iteration followed by a Type (2) iteration. This cycle is repeated as necessary until convergence. Convergence may be achieved during either type of iteration.

Option (2): The timestep begins with one Type (1) iteration followed by two successive Type (2) iterations. This cycle is repeated as necessary until convergence. Convergence may be achieved during any iteration.

Option (3): Same as Option (2), except each Type (1) iteration is followed by three Type (2) iterations. The cycle is completed until convergence.

The performance of each of these options will be compared in the section on performance of the MNR procedure.

The MNR procedure can be easily installed in most fully implicit simulators. It utilizes basic routines already present in most models. The following provisions are necessary:

(1) A routine for calculation of the residual independent of the Jacobian bands.

(2) A band solver which saves the inverted Jacobian for reuse with a new right-hand side vector.

(3) A subprogram for routing execution of the selected option. This routine can easily be written to provide all three MNR options to the user.

Use of MNR with the Substitution of Variables Technique

The three options presented in the previous section require only a single modification to operate in conjunction with the method of substitution of variables. Following each iteration in which phase appearance/disappearance occurs, the MNR procedure is restarted with a full Newton iteration (Type (1)). This is necessary in order to reestablish the Jacobian using the correct sets of primary variables. Once the Jacobian has been updated, execution continues using modified iterations (Type (2)) in accordance with the option selected.

The need to restart in response to changes in cell status may somewhat decrease time savings for the MNR procedure. The optimum solution occurs when phase appearance or disappearance is determined in the first iteration of the timestep, the Jacobian is reset, and convergence is achieved by the first or second MNR cycle.

Performance of the MNR Procedure

Remarkable savings in execution time are possible with the MNR procedure. If the procedure is properly used, time savings will be accompanied by no significant loss in simulation accuracy. Suggestions for proper application of the MNR procedure are included in the examples section of this paper.

With the MNR procedure, the potential for time savings is a function of several characteristics of the simulation problem. Savings will result each time a standard Newton-Raphson iteration is replaced by a shortened MNR iteration. The potential for time savings is increased by the following:

1. Timesteps which require three or more standard Newton-Raphson iterations to achieve convergence. The more iterations required per timestep, the greater opportunity to utilize the shortened MNR iterations.

2. Smaller convergence tolerances. Generally more iterations per timestep are required as tolerances are decreased.

3. Large grid sizes. The larger the Jacobian bandwidth, the more time saved per MNR iteration.

4. When crossing the bubble point, timesteps in which grid blocks switch primary variables only during the first iteration. Because an updated Jacobian is required following any switch in primary variables, the opportunity to use several consecutive MNR iterations is increased when all switching of variables is completed early in the timestep.

Reservoir problems which exhibit the above characteristics can be accelerated 50 percent or more by the MNR procedure. Obviously, gains will decrease as a problem offers less opportunity for the use of shortened MNR iterations.

Three MNR options have been presented. Savings in execution time are typically greatest for Option 3. However, savings are dependent upon the characteristics of the problem. The more MNR iterations replacing standard iterations, the greater the net savings. Option 3 can offer no savings over Option 1 or 2 if the solution for the timestep is gained in two iterations, or if multiple switching of primary variables necessitates frequent updating of the Jacobian.

An ideal application for Option 3 would be a timestep requiring four iterations; one standard Newton-Raphson iteration followed by three MNR iterations. The time savings for a 10x10x1 grid would be approximately 64 percent. The use of Option 1 or 2 for this timestep would require two full Newton-Raphson iterations and two MNR iterations. Time savings for Options 1 and 2 would then be approximately 42 percent.

Option 3 is generally the option of choice. The simulator is set to Option 3. However, timesteps which converge in three or two iterations automatically reduce execution to Options 2 and 1, respectively.

Sometimes the use of the MNR procedure increases the total number of iterations required in a timestep. This occurs because the Jacobian is less frequently updated, and additional iterations are required for convergence. Even in this situation, time savings occur because additional MNR iterations consume relatively little time.

As an example, consider a timestep requiring three standard iterations. If this is replaced by MNR Option 3, one standard iteration and three MNR iterations may be required. For a 10x10x1 grid, savings will be approximately 52 percent.

No significant sacrifice in accuracy accompanies the use of the MNR procedure. For timesteps in which additional iterations are required to achieve convergence, accuracy may actually be increased. In many cases, depending on the number of digits printed, no difference may be evident in the solution. Material balance differences typically occur in the fifth or sixth decimal place, and the material balance may improve slightly in those timesteps which require additional iterations for convergence. In conclusion, the MNR procedure provides significant gains in execution time with no significant loss in simulation accuracy.

EXAMPLES

A series of examples is presented to illustrate the performance of the model. Three problems are used in these examples: a production problem, an injection problem, and a problem in which sequential production and injection occur. The problems are simulated using a 2-D model. Execution times are quoted for an IBM 3090-200 computer. In all runs, convergence is assumed when

$$\frac{\Delta X^{v+1}}{X^{v}} < EPSI \qquad (31)$$

where EPSI equals 10^{-3} to 10^{-4} as specified in each example.

Problem 1: This is a modified version of the reservoir simulation problem presented by Odeh[12]. Changes are made to reduce the solution to 2 dimensions, and only a single production well is used. A 10x10 grid system is utilized. The production well is located in the center of gridblock (1,1), and sandface pressure is specified as 1000 psia for the duration of simulation (see Figure 8). Additional data are summarized in Table 2. All rock and fluid properties are as presented by Odeh. The purpose of Problem 1 is to illustrate the simulation of gas phase appearance.

Problem 2: The purpose of this problem is to demonstrate gas phase disappearance. Reservoir conditions are initially below the bubble point, and water injection occurs in a single well. The same well location, grid system, and rock and fluid properties are used here as for Problem 1, with the following exceptions:

Initial reservoir pressure	3800 psia
Initial values of S_o, S_w, and S_g	0.6000, 0.3775, 0.0225
Initial bubble point pressure	4011.8 psia
Water injection rate	12,500 STBD

Relative permeability data for Problem 2 are presented in Table 3. Stone's model is used with these data for calculation of oil relative permeability.

Problem 3: The purpose of this problem is to demonstrate simulation of both phase appearance and disappearance. Initial reservoir conditions are identical to Problem 2, and the same grid geometry and rock and fluid data are utilized. After 210 days of water injection, the injection well is switched to production, and sandface pressure is specified at 1000 psia for the completion of simulation.

Using Problems 1 through 3, a series of six examples are now presented. Each example will illustrate the performance of different features of the program.

Example 1: Variable Bubble Point Formulation

This example illustrates the stability of the variable bubble point model. A series of runs are presented for Problems 1 through 3. The runs are designed to test the model using both small and large timestep sizes. Comparisons are made between runs on the basis of accuracy and speed of convergence. The following fixed timestep sizes are used:

Problem 1: 10, 50, 100, and 200 days
Problem 2: 10, 50, 100, 200, and 300 days
Problem 3: 10, 50, 100, and 200 days

Total simulation time is 610 days for Problems 1 and 2, and 620 days for Problem 3. In all runs, a 10-day timestep is always used following well openings and well changes. A convergence tolerance of 10^{-3} is used in each run.

Table 4 presents data for the runs. This includes the maximum length timestep (in iterations) and the minimum length timestep for each run. Also, an average timestep length (in iterations) is presented. The data show that more iterations are required per timestep as timestep size increases.

In Problem 1, the free gas phase appears in three reservoir cells during the initial 10-day timestep. After 100 days of production, pressure drawdown causes gas to appear in the remaining 97 reservoir cells. When 100 and 200 day timesteps are used for simulation, a total of 97 cells switch across the bubble point during timestep 2.

In Problem 2, free gas disappears in three reservoir cells during the initial 10-day timestep. After 140 days of injection, increasing pressure causes the free gas phase to disappear in all remaining reservoir cells. Therefore, runs using 200- and 300-day timesteps switch 97 percent of the reservoir cells across the bubble point during timestep 2.

Similar performance is seen in Problem 3 using 200-day timesteps. The free gas phase disappears in 97 reservoir cells during the second timestep of injection (days 10 to 210), and free gas appears in 99 cells during the second timestep of production (days 220 to 420).

Figures 9 through 12 present results from the simulation runs. Figure 9 presents cumulative oil production for the four runs of Problem 1. After 610 days of simulation, cumulative oil production is 5,618,738 and 5,079,081 STB, respectively, for runs using the 10- and 200-day timesteps. This represents a difference of 9.6 percent. At 610 days, pressures in the well block are 1947 and 1966 psia, respectively, for the two runs.

Figure 10 presents pressures in the injection block for Problem 2. After 610 days of simulation, pressures of 9931 and 9862 psia were determined by the 10- and 300-day runs, respectively. Water saturations in the injection block are 0.8314 and 0.8195, respectively, for the two runs.

Figure 11 presents cumulative oil production for Problem 3. Figure 12 presents water saturations in the well block. After 620 days of simulation, cumulative production differs by 1.2 percent (1,648,087 vs. 1,627,681 STB) for the 10- and 200-day timestep runs. Water saturations are 0.4031 and 0.4555 and well block pressures are 2060.6 and 2099.1 psia, respectively, for the two runs.

The 12 runs presented thus far illustrate several characteristics of the variable bubble point model. The program has the ability to utilize large timestep sizes. Major portions of the reservoir may be switched across the bubble point in a single timestep. Reasonable numbers of iterations are used to achieve this performance. From Figures 9 through 12 it can be seen that while the resolution of intermediate details is lost with large timestep sizes, the accuracy of results is not significantly degraded at the completion of simulation.

Example 2: Automatic Timestep Selector

This example illustrates the operation of the automatic timestep selection routine[9]. Two parameters, ε and ω enable the user to adjust the performance of the routine for individual runs. The relative error parameter ε controls the relative magnitude of the time truncation error. The weight ω

determines the emphasis placed upon saturations or pressures for timestep control.

The parameter ε adjusts the lengths of timesteps. Increasing ε increases timestep sizes and therefore time truncation error. Decreasing ε has the opposite effect. Functional values for ε range from 0.05 to 0.50. From our experience, values in the range of 0.20 to 0.35 are appropriate for black oil simulation. Larger values may be appropriate when resolution may be exchanged for speed of execution.

In the examples presented here, the value of ω is set to 2.0. Sammon and Rubin[9] recommend using values of 1 to 2. While small values of ω increase emphasis on changes in P_o and R_s, large values place emphasis on saturations. This is appropriate for water injection in Problem 3.

Problem 3 is used to illustrate performance of the automatic timestep selection routine. Runs are made for approximately 325 days using a convergence tolerance of 10^{-3}. In Table 5 seven runs are presented for values of ε ranging from 0.10 to 0.40 in increments of 0.05. A timestep size of 2.5 days is used for well openings and well changes. All other timesteps are calculated by the automatic timestep routine. Table 5 presents the maximum, minimum, and average timestep length (in days and iterations), and the total number of timesteps and iterations required per run.

The data present a clear view of the performance of the automatic timestep selector. The following observations can be made: timestep sizes, and therefore time truncation errors, increase with the magnitude of ε; the average number of iterations required per timestep increases with ε; iterations per timestep do not exceed four in any of the runs presented. The last observation is a key to the success of the timestep selector. As stated by Sammon and Rubin, when using the selector, the number of iterations per timestep is kept small, and this time savings allows for the use of additional timesteps. Smaller timestep sizes can then be used, and this increases simulator accuracy.

Example 3: Estimation of Results for Succeeding Timesteps

This example demonstrates the usefulness of the estimation algorithm for predicting phase appearance and disappearance and the values of primary variables for succeeding timesteps. Problems 1 and 2 were run using the automatic timestep selector. The estimation algorithm was placed in effect whenever consecutive timestep sizes did not differ greatly as determined by the following criterion[9]:

$$\frac{2}{3} < \frac{\Delta t^{n+2}}{\Delta t^{n+1}} < \frac{3}{2} \qquad (32)$$

Results are shown in Table 6. Problem 1 was simulated for 14 timesteps. The estimation algorithm was in effect for 12 timesteps, including 8 of the 10 steps in which gas phase appearance occurred. Table 6 presents the execution time for this run and a control run in which the estimation algorithm was not utilized. Results show a 21.5 percent gain in speed of execution.

Problem 2 was simulated for 23 timesteps. The estimation algorithm was in effect for 21 timesteps, including 16 of the 18 steps in which gas phase appearance occurred. In Table 6, comparisons are presented between this run and a control run. Results show that an 18.9 percent gain in speed of execution was obtained using the estimation algorithm.

Example 4: MNR Procedure

Problems 1 and 2 were simulated using the three MNR options. A fixed timestep size of 10 days and a convergence tolerance of 10^{-4} were used in all runs.

Results for Problem 1 are presented in Table 6. Option 3 is presented in comparison with the standard Newton-Raphson procedure (designated Option 0). For the 15 timesteps shown, overall savings in execution time were 30.4 percent. Crossing the bubble point (first 10 timesteps), savings were 20.2 percent. For execution below the bubble point (timesteps 11 through 15), savings were 56.3 percent.

When crossing the bubble point, often the switching of primary variables was spread over several iterations of each timestep, and this prevented maximum use of shortened MNR iterations. Blocks switching back and forth across the bubble point completely prevented the use of MNR in timesteps 6 and 9. After the bubble point was crossed (timestep 11), two MNR and one standard iterations were used per timestep. This corresponds to the execution of Option 2. Although Option 3 was selected, convergence occurred with only two MNR iterations, preventing full use of Option 3.

In 15 timesteps, the MNR procedure required 57 total iterations compared to 54 for the standard procedure. Cumulative oil production and well block pressure are shown at 150 days of simulation. Pressures are identical for the number of digits printed, and oil production shows a difference of 5.6 STB or 2.9×10^{-4} percent.

Results for Problem 2 are shown in Table 8. Again Option 3 is compared with the standard Newton-Raphson procedure. Time savings for 20 timesteps of simulation are 45.4 percent. This represents a savings of 42.4 percent in crossing the bubble point (timesteps 1 through 14) and a savings of 57.4 percent for simulation above the bubble point.

When crossing the bubble point, the MNR procedure was used more extensively in Problem 2 than in Problem 1. This occurred because in Problem 2 most of the switching of primary variables occurred during the first iterations of the timesteps. Less frequent updating of the Jacobian was therefore necessary, and more frequent use could be made of shortened MNR iterations.

A comparison for Problem 2 shows that both MNR Option 3 and the standard Newton-Raphson procedure required exactly the same number of iterations to complete 20 timesteps. Calculated values are shown in Table 8 for pressure and water saturation in the injection block at timestep 20. Values are identical for the two methods for the number of digits printed.

Results thus far have been presented only for MNR Option 3. However, in most of the timesteps shown,

convergence occurred with only one or two consecutive MNR iterations. In these situations, execution was reduced to Options 1 and 2, respectively. This is typical of most problems. For this reason, it is recommended that black oil models be set to MNR Option 3 and allow early convergence and the switching of primary variables to reduce execution to Options 1 and 2 as necessary. Whenever full execution of Option 3 is possible, it will be used by the simulator, and maximum time savings will result.

Table 9 compares the three MNR options for Problems 1 and 2. The simulator is set to a specific option and run for 200 seconds. Option 3 clearly outperforms the others. At times, Option 2 approaches the performance of Option 3. This occurs when execution of Option 3 is limited by convergence and the switching of primary variables.

Example 5: Interaction Between MNR and the Automatic Timestep Selector

A series of runs was made to determine the effect of the MNR procedure on the automatic timestep selector. In theory, the vectors $\dot{X}_b^{n+1}$ and $\dot{X}_c^{n+1}$ used in the selection routine should be calculated using values obtained after convergence of each timestep. In practice, these vectors are determined using values available from the calculation of the last full Jacobian. This implies that for option 1, values two iterations previous to the end of the timestep are used to calculate $\dot{X}_b^{n+1}$ and $\dot{X}_c^{n+1}$. For Options 2 and 3, values three and four iterations, respectively, previous to the end of the timestep are used to calculate the vectors.

To gain a quantitative measure of the effect of this practice, Problems 1 and 2 were run using the three MNR options and the standard Newton-Raphson procedure. Simulation was stopped at approximately 200 days. The automatic timestep selector was used for all runs. Results are presented in Table 10.

Results shown in Table 10 indicate that small variations can be expected in timestep sizes when using the MNR procedure. In the two problems, variations in timestep sizes between the options never exceeded 0.8 days. To avoid potential variations in timestep sizes, a conservative approach would be to use MNR Options 1 or 2 instead of Option 3 in conjunction with the automatic timestep selection routine.

Example 6: Interaction Between MNR and the Estimation Algorithm

This example demonstrates the combined performance of the MNR procedure and the estimation algorithm used for prediction of results for succeeding timesteps. Problems 1 and 2 are run as in Example 3 using the three MNR options and the standard Newton-Raphson procedure. Execution times are presented for these eight runs in Table 11.

Comparing Options 2 and 3, it is interesting to note that Option 2 produced greater time savings in Problem 1, and Option 3 produced greater savings in Problem 2. Normally, Option 3 would be expected to outperform Option 2. In Problem 1, Option 3 required extra iterations in several timesteps while crossing the bubble point. These were timesteps in which values four iterations previous to convergence were used to calculate the vector X_b^{n+1} (see example 5). The vector X_b^{n+1} is of prime importance in the estimation algorithm, and accurate values will not always be available using MNR Option 3. Therefore, prediction of phase appearance and disappearance is not reliable using this option. For this reason, it is recommended that only MNR Options 1 and 2 be used with the estimation algorithm. Option 1 would provide the greatest reliability.

It is interesting to compare total time savings resulting from the use of MNR Option 2 and the estimation routine. For Problem 1, 142.16 seconds was required when using only the automatic timestep selector and the standard Newton-Raphson procedure. Using MNR Option 2, the automatic timestep selector, and the estimation algorithm reduces execution time to 75.88 seconds for a savings of 46.6 percent. Without the estimation algorithm, savings would be only 27.3 percent. For Problem 2, 282.52 seconds were required for standard execution. Using MNR Option 2, the timestep selector, and the estimation algorithm reduces execution time to 129.02 seconds for a savings of 54.3 percent. Without the estimation algorithm, savings would be only 38.7 percent. For longer simulation runs with relatively less switching of variables, time savings would increase over the values shown as more advantage could be gained from the MNR procedure.

SUMMARY

(1) A fully implicit, variable bubble point black oil model is presented. The program uses the method of substitution of variables for modeling appearance and disappearance of the free gas phase. An outline of formulations, switching schemes and techniques for acceleration of convergence are presented. Tests show the stability and versatility of the model, including its ability to accommodate large timestep sizes, such that major portions of the reservoir can pass across the bubble point in a single timestep.

(2) Modifications are presented to adapt the automatic timestep selector of Sammon and Rubin to variable bubble point simulation. Tests show the routine performs effectively in conjunction with the black oil model. An estimation algorithm, built into the routine, can predict phase appearance and disappearance in reservoir cells, and can accelerate execution across the bubble point.

(3) A modified Newton-Raphson procedure (MNR) is presented. Three versions of the procedure are described and tested. Large gains in execution time can accompany use of MNR. Savings exceeding 50 percent are demonstrated for MNR Option 3. Virtually no significant loss in accuracy occurs with proper use. In conjunction with the automatic timestep selection routine, MNR Options 1 or 2 are recommended. These same Options are also recommended for use with the estimation algorithm. Time savings exceeding 50 percent are demonstrated when MNR Option 2 is used with the automatic timestep selector and the estimation algorithm.

(4) Possibilities exist for higher order MNR versions for use in simulators which require in excess of four iterations per timestep. These versions would use four or more shortened MNR iterations following each standard Newton-Raphson iteration.

NOMENCLATURE

A = Accumulation vector

ARGE = Add to the residual of the gas equation

AROE = Add to the residual of the oil equation

ARWE = Add to the residual of the water equation

B = Formation volume factor

C = Compressibility

DA = Accumulation Jacobian $(\frac{\partial A}{\partial X})$

DF = Flow Jacobian $(\frac{\partial F}{\partial X})$

e = Primary reservoir variable error vector

EPSGAS = 10^{-11}

EPSI = 10^{-3} to 10^{-4}

EPSRST = 10^{-6}

F = Flow vector

INDC1 = Indicator used with interblock flow and source terms

INDC2 = Indicator used with accumulation terms

J = Jacobian

m = Number of primary equations per reservoir cell (3)

ΔM = Change in mass during Δt

N = Number of cells in the reservoir

P_b = Bubble point pressure

P_o = Oil pressure

Q = Source or sink term

R = Residual vector

R_s = Solution gas oil ratio

S = Saturation

Δt = Timestep length

V_b = Bulk volume

X = Solution vector

ΔX = Change in solution vector

$\dot{X}_b$ = Backward difference derivative vector for X

$\dot{X}_c$ = Correct derivative vector for X

α = Weight

ε = Relative error parameter

λ = Transmissibility

ϕ = Porosity

$\Delta\Phi$ = Potential difference

ω = Weighting fraction

Operators

Δ = Difference operator

Subscripts

b = Bubble point

g = Gas

i = Equation

j = Reservoir cell number

o = Oil

t = Time

w = Water

Superscripts

n = Time level

v = Iteration level

* = Difference takes the form $(P_o^{n+1}-P_{o_b}^{n})$ or $(R_s^{n+1}-R_{s_b}^{n+1})$

ACKNOWLEDGEMENTS

This research was partially supported by a grant from National Fuel Gas Supply Corporation. Appreciation is expressed to Dr. J. Abou-Kassem for his contributions.

REFERENCES

1. Forsyth, P., Jr., and Sammon, P. H.: "Gas Phase Appearance and Disappearance in Fully Implicit Black Oil Simulation," SPEJ (Oct. 1984) 505-507.

2. Ponting, D. K., et al.: "An Efficient Fully Implicit Simulator," SPEJ (June 1983) 544-552.

3. Stright, D. H., Jr., et al.: "Carbon Dioxide Injection into Bottomwater, Undersaturated Viscous Oil Reservoirs," JPT (Oct. 1977) 1248-1258.

4. Thomas, L. K., et al.: "Reservoir Simulation of Variable Bubble-Point Problems," SPEJ (Feb. 1976) 10-16.

5. Aziz, K. and Settari, A.: Petroleum Reservoir Simulation, Applied Science, London (1979).

6. Coats, K. H.: "A Highly Implicit Steamflood Model," SPEJ (Oct. 1978) 369-383.

7. Forsyth, P., Jr., Rubin, B., and Vinsome, P. K. W.: "The Elimination of the Constraint Equation and Modeling of Problems with a Non-Condensable Gas in Steam Simulation," J. Can. Pet. Tech. (Oct.-Dec. 1981) 63-68.

8. Lutchmansingh, P. M.: "Mathematical Simulation of the Polymer Flooding Process," Ph.D. Thesis, Pennsylvania State University, University Park, PA (1987).

9. Sammon, P. H. and Rubin, B.: "Practical Control of Timestep Selection in Thermal Simulation," paper SPE 12268, presented at the Reservoir Simulation Symposium, San Francisco, CA, Nov. 15-18, 1983.

10. King, G. R., Ertekin, T. and Schwerer, F. C.: "Numerical Simulation of the Transient Behavior of Coal-Seam Degasification Wells," SPE Form. Eval. (April 1983) 165-183.

11. Au, A. D. K., et al.: "Techniques for Fully Implicit Reservoir Simulation," paper SPE 9302 presented at the 1980 SPE Annual Technical Conference and Exhibition, Dallas, Sept. 21-24.

12. Odeh, A. S.: "Comparison of Solutions to a Three-Dimensional Black-Oil Reservoir Simulation Problem," JPT (Jan. 1981) 13-25.

TABLE 1.a - EXECUTION TIMES FOR THE STANDARD NEWTON-RAPHSON PROCEDURE

PROGRAM SEGMENT	TIME REQUIREMENTS FOR DIFFERENT SIZE GRIDS (sec x 10-3) 5x5x1	8x8x1	10x10x1
Construction of the Jacobian Bands	52	145	235
Loading the Envelope	57	70	82
Inversion of Jacobian	142	920	2229
Solution of Equations	38	148	285
	289	1283	2831

TABLE 1.b - EXECUTION TIMES FOR THE MODIFIED NEWTON-RAPHSON PROCEDURE

PROGRAM SEGMENT	TIME REQUIREMENTS FOR DIFFERENT SIZE GRIDS (sec x 10-3) 5x5x1	8x8x1	10x10x1
Construction of the Residual	20	62	95
Solution of Equations	38	148	285
	58	210	380

Values are for standard ordering with matrix inversion by Gaussian elimination.

TABLE 2 - DATA FOR PROBLEM 1

Simulation	2 Dimensional
Grid System	10 x 10
Block Dimensions, ft	1000 x 1000 x 20
X and Y Permeabilities, md	500, 500
Initial Reservoir Pressure, psia	4800
Initial Saturations, So,Sw,Sg	0.88, 0.12, 0.0
Initial Bubble Point Pressure, psia	4014.7
Well Block Location	1, 1
Sandface Production Pressure, psia	1000
Well Diameter, ft	0.50
Water Viscosity, cp	1.0

TABLE 3 - RELATIVE PERMEABILITY DATA FOR PROBLEMS 2 AND 3

Sw	KRW	KROW	Sw + So	KRG	KROG
0.120	0.00	1.00	0.120	0.984	0.0000
0.140	0.28571	0.971429	0.150	0.980	0.0000
0.160	0.57143	0.942857	0.300	0.940	0.0000
0.180	0.085714	0.914286	0.400	0.870	0.0001
0.220	0.142857	0.857143	0.500	0.720	0.0010
0.320	0.285714	0.714286	0.550	0.600	0.0100
0.420	0.428571	0.571429	0.600	0.410	0.0210
0.560	0.628571	0.371429	0.700	0.190	0.0900
0.700	0.828571	0.171429	0.750	0.125	0.2000
0.760	0.914286	0.085714	0.800	0.075	0.3500
0.780	0.942857	0.057143	0.880	0.025	0.7000
0.800	0.971429	0.028571	0.950	0.005	0.9800
0.820	1.00	0.00	0.980	0.000	0.9970
			0.990	0.000	1.0000
			1.000	0.000	1.0000

TABLE 4 - DATA FOR EXAMPLE 1

PROBLEM 1:

TIMESTEP SIZE (da)	MAXIMUM ITERATIONS	MINIMUM ITERATIONS	AVERAGE FOR SIMULATION
10	4	2	2.1
50	5	2	3.2
100	6	3	3.5
200	6	3	4.3

PROBLEM 2:

10	5	2	2.4
50	5	3	3.4
100	7	3	4.2
200	7	5	5.6
300	8	6	7.0

PROBLEM 3:

10	4	2	2.6
50	5	2	3.5
100	7	3	4.5
200	7	4	5.6

TABLE 5 - DATA FOR EXAMPLE 2

	TIMESTEP LENGTH (da)			ITERATIONS PER TS			TOTAL	
EPS	MAX	MIN	AVE	MAX	MIN	AVE	TS	ITR
0.10	5.88	1.30	4.21	4	2	2.53	76	192
0.15	8.55	1.94	5.98	4	2	2.74	54	148
0.20	11.10	2.59	7.99	4	2	2.83	41	116
0.25	13.26	3.27	9.45	4	2	2.97	34	101
0.30	16.31	3.93	11.29	4	2	3.17	29	92
0.35	19.07	4.58	13.28	4	2	3.36	25	84
0.40	23.84	5.24	15.07	4	2	3.59	22	79

EPS = EPSILON ITR = ITERATIONS TS = TIMESTEPS

SPE 16342

TABLE 6 - DATA FOR EXAMPLE 3

PROBLEM 1:	TIMESTEPS SIMULATED	TIMESTEPS USING THE ESTIMATION ALGORITHM	EXECUTION TIME (sec)
ESTIMATE ON	14	12	111.52
ESTIMATE OFF	14	0	142.16
PROBLEM 2:			
ESTIMATE ON	23	21	229.11
ESTIMATE OFF	23	0	282.52

TABLE 7 - DATA FOR EXAMPLE 4

PROBLEM 1:

	STANDARD NEWTON-RAPHSON			MODIFIED NEWTON-RAPHSON		
TS	FULL	TIME	BLOCKS	FULL	MNR	TIME
1	5	13.878	1	4	3	12.237
2	5	13.894	3	3	3	9.496
3	4	11.133	4	2	2	6.491
4	4	11.147	3	3	1	8.923
5	3	8.399	6	2	1	6.100
6	3	8.404	5	3	0	8.400
7	4	11.214	15	3	1	8.800
8	4	11.254	21	3	1	8.858
9	4	11.340	27	4	0	11.601
10	3	8.543	15	2	1	6.920
11	3	8.551	0	1	2	3.764
12	3	8.582		1	2	3.776
13	3	8.752		1	2	3.780
14	3	8.779		1	2	3.782
15	3	8.548		1	2	3.781
	54	152.418	100	34	23	106.079
				57		

	STANDARD N-R	MNR
CUMULATIVE PRODUCTION (STB)	1963144.9	1963150.5
PRESSURE IN THE WELL BLOCK (PSIA)	2352.4	2352.4

TS = TIMESTEP NUMBER (FIXED TIME STEP = 10 DAYS)
FULL = STANDARD NEWTON-RAPHSON ITERATIONS
MNR = MODIFIED NEWTON-RAPHSON ITERATIONS
TIME = EXECUTION TIME REQUIRED FOR THE TIMESTEP (SECONDS)
BLOCKS = NUMBER OF GRID BLOCKS WHICH CROSS THE BUBBLE POINT DURING THE TIMESTEP

TABLE 8 - DATA FOR EXAMPLE 4

PROBLEM 2:

	STANDARD NEWTON-RAPHSON			MODIFIED NEWTON-RAPHSON		
TS	FULL	TIME	BLOCKS	FULL	MNR	TIME
1	6	17.089	3	3	3	9.765
2	5	14.263	3	2	3	6.913
3	5	14.269	2	2	3	6.903
4	5	14.233	5	2	3	6.901
5	4	11.389	2	2	2	6.505
6	5	14.220	5	2	3	6.895
7	5	14.191	2	2	3	6.876
8	5	14.169	6	2	3	6.875
9	5	14.181	7	5	0	14.169
10	5	14.164	4	2	3	6.850
11	5	14.142	11	3	2	9.269
12	5	14.079	22	3	2	9.226
13	5	14.004	15	3	2	9.177
14	6	16.742	13	3	3	9.524
15	3	8.391	0	1	2	3.574
16	3	8.394		1	2	3.577
17	3	8.404		1	2	3.570
18	3	8.410		1	2	3.573
19	3	8.404		1	2	3.575
20	3	8.394		1	2	3.582
	89	251.532	100	42	47	137.299
				89		

	STANDARD N-R	MNR
WATER SATURATION IN WELL BLOCK	0.8196	0.8196
PRESSURE IN THE WELL BLOCK (PSIA)	6031.5	6031.5

TS = TIMESTEP NUMBER (FIXED TIME STEP = 10 DAYS)
FULL = STANDARD NEWTON-RAPHSON ITERATIONS
MNR = MODIFIED NEWTON-RAPHSON ITERATIONS
TIME = EXECUTION TIME REQUIRED FOR THE TIMESTEP (SECONDS)
BLOCKS = NUMBER OF GRID BLOCKS WHICH CROSS THE BUBBLE POINT DURING THE TIMESTEP

TABLE 9 - DATA FOR EXAMPLE 4

MNR OPTION IN EFFECT	PROBLEM 1: TOTAL TIMESTEPS	PROBLEM 2: TOTAL TIMESTEPS
0	20	13
1	28	22
2	39	30
3	40	36

TABLE 10 - DATA FOR EXAMPLE 4

PROBLEM 1:

MNR OPTION IN EFFECT	DAYS OF SIMULATION	NUMBER OF TIMESTEPS CALCULATED USING EACH MNR OPTION MNR = 0,	1,	2,	3,
0	202.25	13	0	0	0
1	202.27	6	7	0	0
2	202.03	6	3	4	0
3	196.93	3	4	2	4

PROBLEM 2:

0	203.42	22	0	0	0
1	202.53	15	7	0	0
2	204.62	7	0	15	0
3	204.60	0	2	14	6

TABLE 11 - DATA FOR EXAMPLE 5

PROBLEM 1:

MNR OPTION IN EFFECT	TOTAL EXECUTION TIME (sec)
0	111.52
1	86.41
2	75.88
3	78.15

PROBLEM 2:

0	229.11
1	156.13
2	129.02
3	121.68

SPE 16342

BLOCK CONDITIONS	CASE #	INDC2	VARIABLES	EQUATION(S)
FREE GAS IS PRESENT	Case 1	1	Sw, So, Po	13
FREE GAS DISAPPEARING	Case 2	1 → 2	Rs, So, Po	14 - 17
NO FREE GAS IS PRESENT	Case 3	3	Rs, So, Po	18
FREE GAS IS APPEARING	Case 4	3 → 4	Sw, So, Po	19 - 21

During a single timestep, switches are only permitted between Case 1 and Case 2 or between Case 3 and Case 4.

Fig. 1—Derivatives of the accumulation terms.

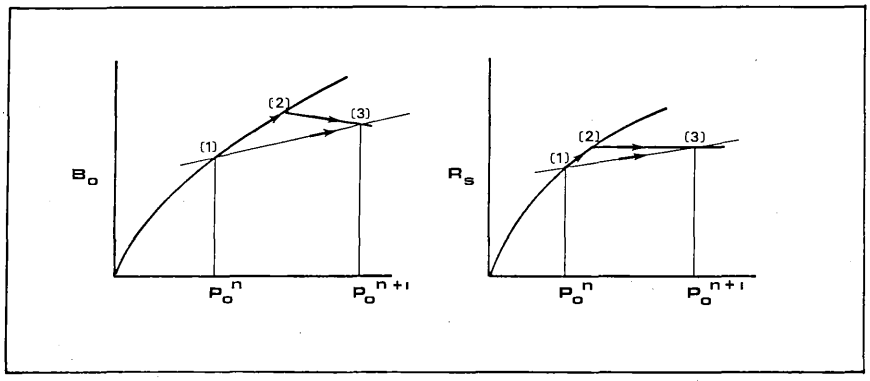

Fig. 2—Case 2—B_o and R_s—gas phase disappearance.

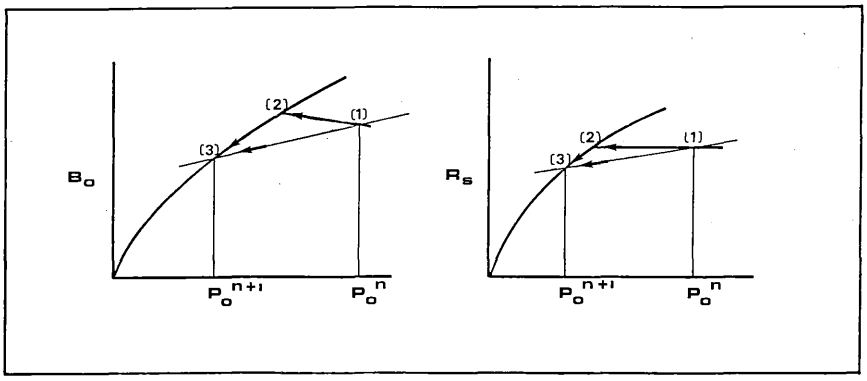

Fig. 3—Case 4—B_o and R_s—gas phase appearance.

CENTRAL BLOCK CONDITION & INDC1		UPSTREAM BLOCK	INDC1 IN UPSTREAM BLOCK	VARIABLES
FREE GAS IS PRESENT (PRESSURE IS BELOW Pb)	1	CENTRAL	1	Sw,So,Po
	1	ADJACENT	1	Sw,So,Po
	1	ADJACENT	0	Rs,So,Po
NO FREE GAS PRESENT (PRESSURE IS ABOVE Pb)	0	CENTRAL	0	Rs,So,Po
	0	ADJACENT	0	Rs,So,Po
	0	ADJACENT	1	Sw,So,Po

During each iteration, appropriate equations are selected based on block conditions.

Fig. 4—Derivatives of the interblock flow terms.

CONDITIONS IN WELL BLOCK	INDC2	VARIABLES	ORDER OF EQUATIONS
FREE GAS IS PRESENT (PRESSURE IS BELOW Pb)	1	Sw, So, Po	WATER, OIL, GAS
NO FREE GAS PRESENT (PRESSURE IS ABOVE Pb)	0	Rs, So, Po	GAS, OIL, WATER

During each iteration, appropriate equations are selected based on block conditions.

Fig. 5—Derivatives of the source terms.

FREE GAS IS PRESENT IN THE RESERVOIR CELL

```
IF (Sg > 0.0) THEN
   INDC1 = 1
   INDC2 = 1
   Rs_b^n = Rs^n + Sg^n*Bo^n/(So^n*Bg^n)
   P_b^n  = Po(Rs_b^n)
   Bo_b^n = Bo(P_b^n)
ENDIF
```

NO FREE GAS PRESENT IN THE RESERVOIR CELL

```
IF (Sg = 0.0) THEN
   INDC1 = 0
   INDC2 = 3
   Rs_b^n = Rs^n
   P_b^n  = Po(Rs_b^n)
   Bo_b^n = Bo(P_b^n)
ENDIF
```

Fig. 6—Initialization at the beginning of a timestep.

SWITCHES - GAS PHASE APPEARANCE

```
Rs(Po^n+1) = TABLE VALUE OF Rs AT Po^n+1
IF (Rs^n+1 > (Rs(Po^n+1) - EPSRST)) THEN
   INDC1 = 1
   IF (INDC2 = 3) THEN INDC2 = 4
   IF (INDC2 = 2) THEN INDC2 = 1
ENDIF
```

SWITCHES - GAS PHASE DISAPPEARANCE

```
Sg^n+1  = 1.0 - Sw^n+1 - So^n+1
IF (Sg^n+1 < EPSGAS) THEN
   INDC1 = 0
   IF (INDC2 = 4) THEN INDC2 = 3
   IF (INDC2 = 1) THEN INDC2 = 2
   So^n+1 = 1.0 - Sw^n+1
   Rs^n+1 = Rs(Po^n+1) + Sg^n+1*Bo(Po^n+1)/(So^n+1*Bg(Po^n+1))
   Sg^n+1 = 0.0
ENDIF
```

Fig. 7—Switching—phase appearance/disappearance.

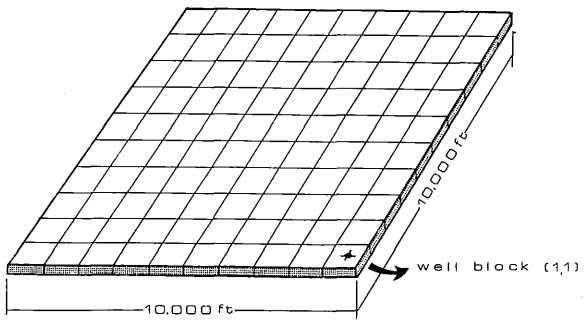

Fig. 8—Description of the reservoir grid for Problems 1, 2, and 3.

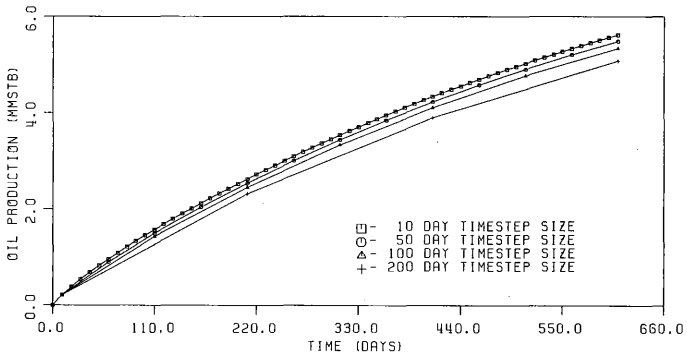

Fig. 9—Cumulative oil production for Problem 1.

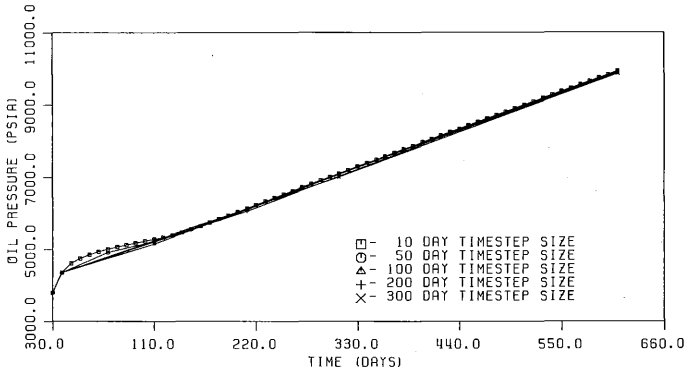

Fig. 10—Well block pressure for Problem 2.

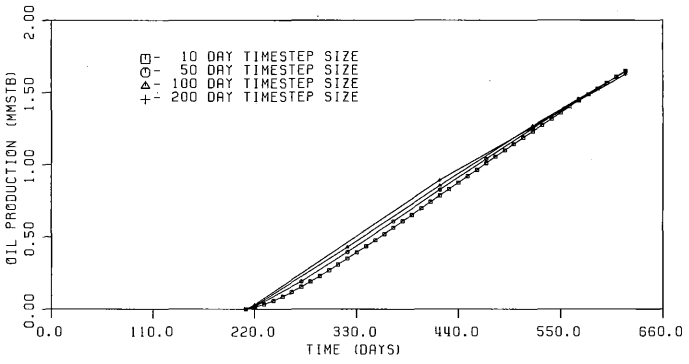

Fig. 11—Cumulative oil production for Problem 3.

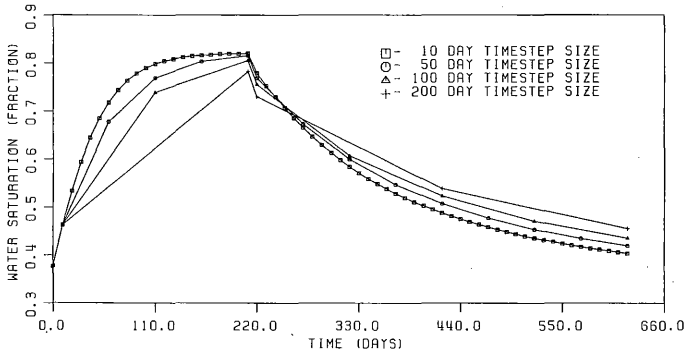

Fig. 12—Well block water saturation for Problem 3.